Exploring fibre orientation dispersion in the corpus callosum: Comparison of dMRI, PLI and Histology

Submission Number:

4255

Submission Type:

Abstract Submission

Authors:

Jeroen Mollink[1,2], Michiel Kleinnijenhuis[1], Stamatios N. Sotiropoulos[1], Michiel Cottaar[1], Anne-Marie van Cappellen van Walsum[2], Menuka Gamarallage[3], Olaf Ansorge[3], Saad Jbabdi[1], Karla Miller[1]

Institutions:

[1]FMRIB centre, University of Oxford, Oxford, United Kingdom, [2]Department of Anatomy, Radboud UMC, Nijmegen, Netherlands, [3]Department of Clinical Neurology, University of Oxford, Oxford, United Kingdom

Introduction:

While increasingly sophisticated models for diffusion-weighted MRI (dMRI) enable the reconstruction of crossing fibres in the brain, less attention has been paid to more subtle fibre architecture within a voxel such as fanning. These features have potential to improve current tractography paradigms or serve as markers of local fibre coherence[1,2]. We present a multimodal study comparing fibre orientation dispersion derived from a parametric dispersion model[3] in dMRI to equivalent models in microscopy images. Here, we use the corpus callosum (CC), a frequent test-bed for crossing fibre models, which is often assumed to be highly coherent pathway in which fibres are organized parallel. Our results, however, reveal a considerable amount of orientation dispersion, in agreement with previous literature[4,5].

Methods:

Three 5 mm coronal slabs (S1-3) including the CC and the cingulate gyri were excised from formalin fixed brains. The pipeline for each sample can be found in Figure 1. **MRI:** Imaging was performed on a 9.4T preclinical Varian MR system using a diffusion-weighted spin echo sequence. 120 gradient directions (240 in sample S1) and 4 non-diffusion weighted images were acquired for two shells (b=2500,5000 s/mm2). Additional parameters: TR=2.4s, TE=29ms, δ=6ms, Δ=16ms and 0.4 mm isotropic voxels. **PLI:** Samples were frozen before cutting them serially in 60µm sections. Sections were imaged with a polarizing microscope. Raw PLI images were acquired and processed according to existing protocols[6]. **Histology:** Samples were embedded in paraffin and cut at 6µm thickness. Sections were stained for proteolipidprotein (PLP, myelin marker) and glial-fibrillary-acidic-protein (GFAP, astroglial marker).

The dispersion model was fitted to the MR-data that yielded a Bingham distribution for the anisotropic volume fraction of the diffusion signal. As PLI already provides high-resolution fibre orientation maps (FOM), a Bingham distribution could be directly fitted to fibre orientation distributions. Texture analysis revealed local fibre orientations from myelin (structure tensor[4]) and glia processes (discrete fourier analysis[7] after color-based segmentation) in the histological images to which again a Bingham distribution was fitted. Dispersion values were extracted from the Bingham distributions and correlated between the modalities.

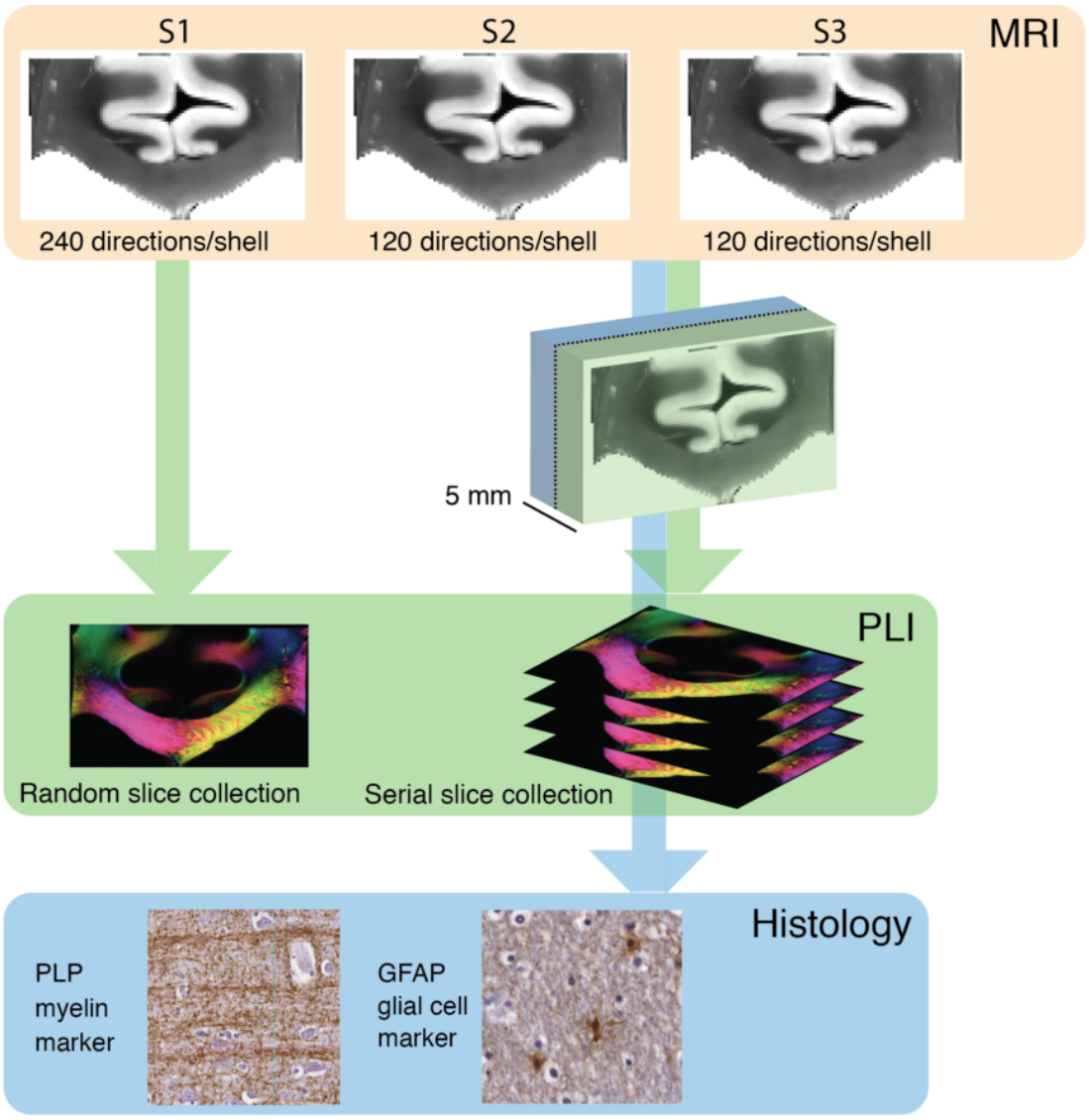

Figure 1. Imaging pipeline. No histological data was collected from S1. S2 and S3 were processed similarly, i.e. by splitting the sample after MR scanning in a PLI part and a histology part. Additionally, PLI slices for S2 and S3 were collected in a serial manner that allows 3D reconstruction.

Results:

Broadly similar patterns can be recognized in the orientation dispersion maps between dMRI, PLI and histology, with high dispersion in crossing fibre regions like the centrum semiovale and less dispersion in the CC (Figure 2). However, even a coherent white matter bundle as the CC is estimated to exhibit a considerable amount of dispersion. Regional quantification the dispersion profiles in the CC resulted in great correspondence between PLI, histology and the dMRI (Figure 3). In terms of absolute values, the diffusion-derived estimates match the histology dispersion much better. Figure 4 illustrates some of the sources that could contribute to fibre orientation dispersion estimated by MR models. In some regions of the CC, there are significant glial cell processes with consistent orientation perpendicular to the main fibre orientation. The lateral areas with visible striping patterns in PLI appear to have local fibre bundles running at large angles (~45 degrees) in close proximity.

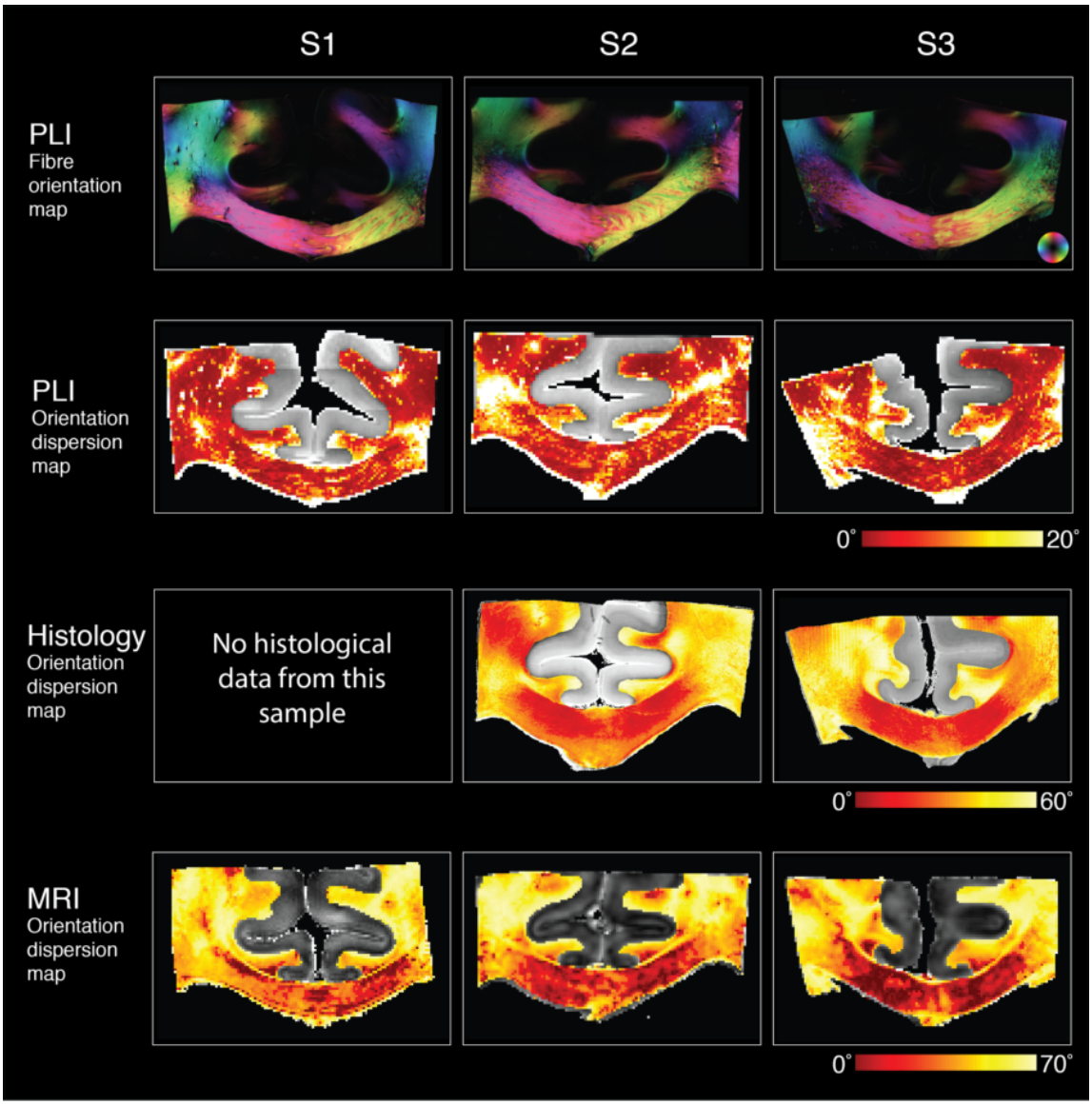

Figure 2. Fibre orientation and dispersion maps. PLI fiber orientation maps are shown in HSV colorspace, with the hue channel coding for the in plane fiber orientation. Fibre orientation dispersion maps represent the angular spread of fibres when 95% of the samples are included in the Bingham distribution. They are shown for PLI, histology and dMRI.

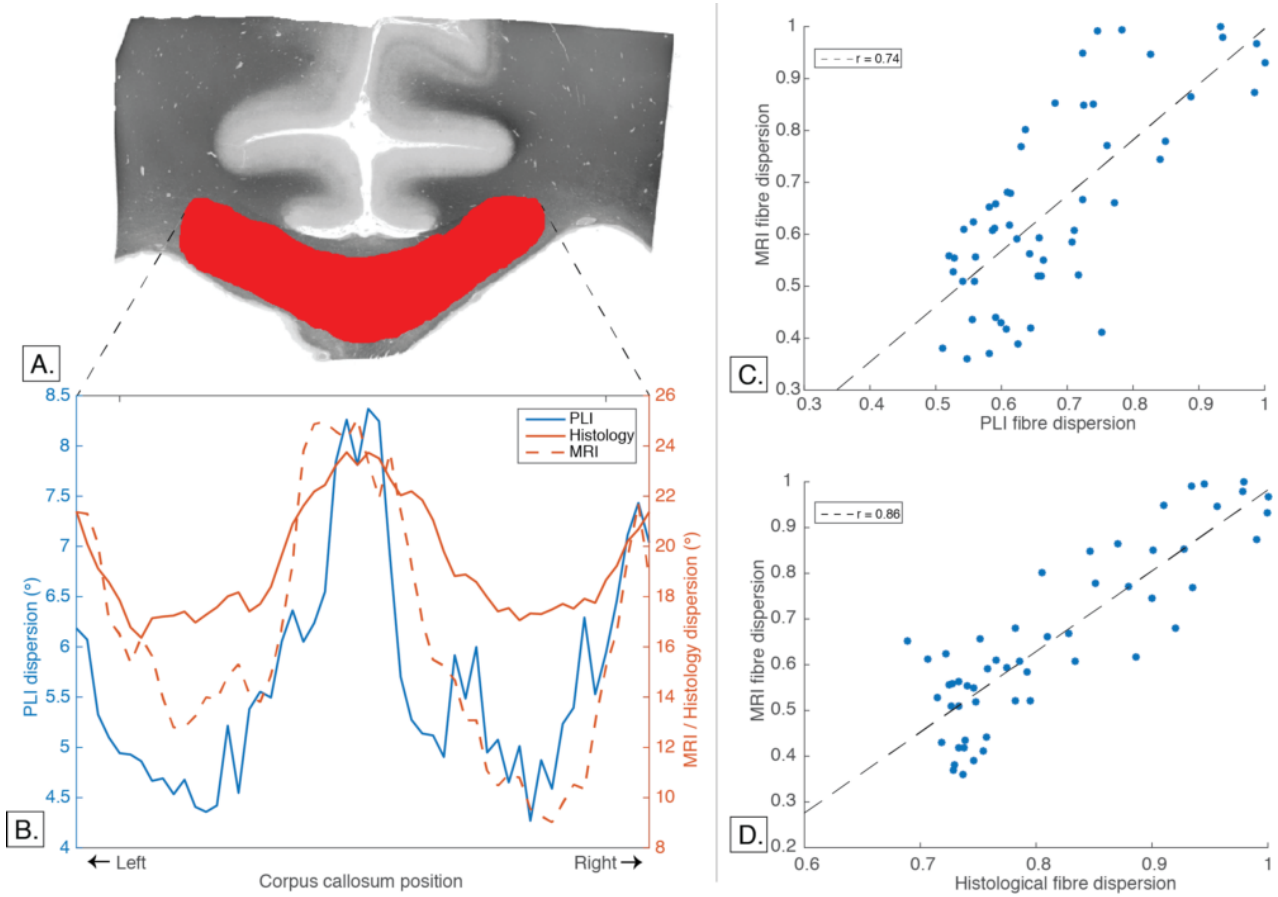

Figure 3. Fibre orientation dispersion in the corpus callosum demonstrated with PLI, histology and dMRI using a parametric dispersion model. **A)** Corpus callosum mask. **B)** Fibre orientation dispersion profiles along the corpus callosum. **C)** Correlation between the relative orientation dispersion profiles for PLI and dMRI. **D)** Similarly as in **C)** but for histology instead of PLI.

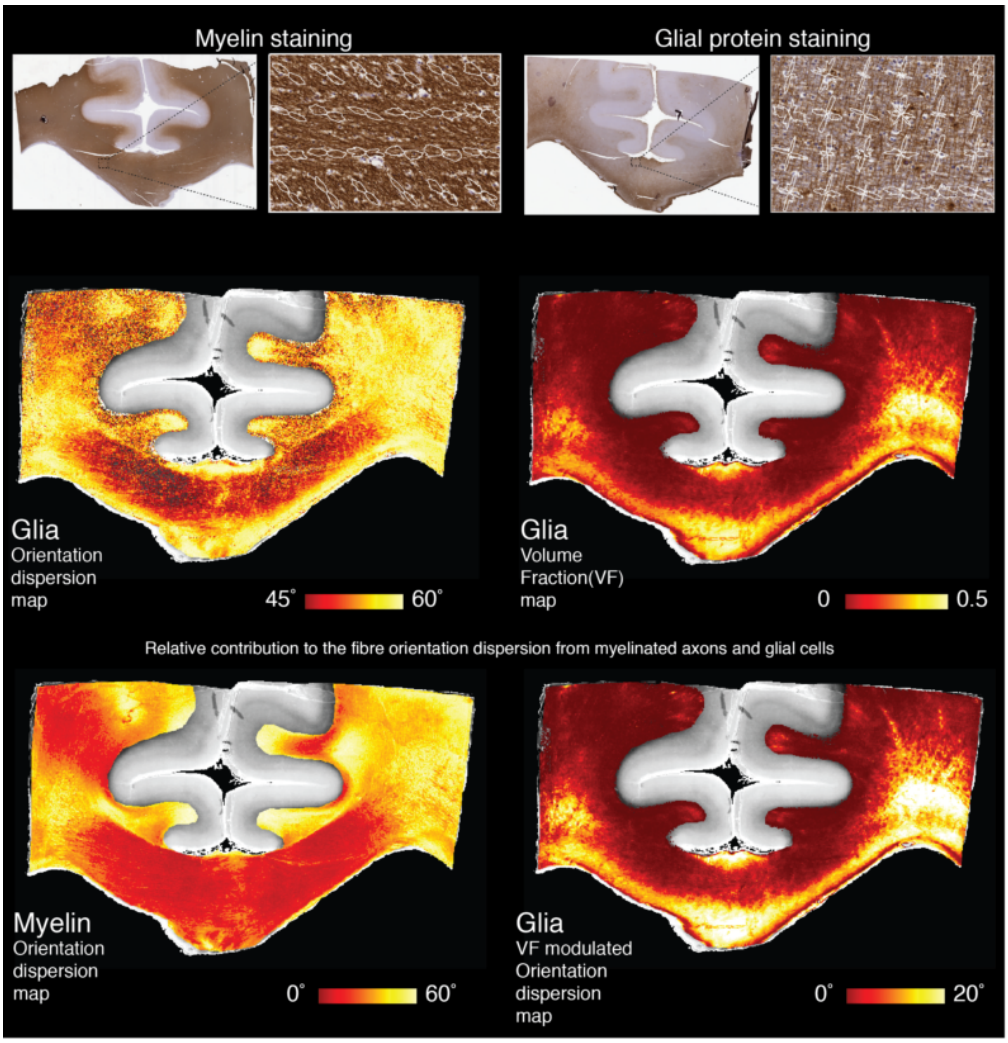

Figure 4. **Top:** Sources of dispersion in the corpus callosum demonstrated with histological stainings for myelin proteins and glial cell proteins. Local fibre bundles at large angles(~45 degrees) are running in close proximity, even in an often assumed to be coherent structure as the CC. The close-up of the glial cell staining demonstrates fibre crossings of astrocyte processes with underlying axons. **Middle:** Large fibre orientation dispersion values are observerd for glial cells proccesses as they are mainly randomly distributed. However, because the observed volume fraction is low for most of the areas in the sample, their contribution to total fibre orientation dispersion is low as well in these areas. **Bottom:** Relative contributions from myelin and glia to the fibre orientation dispersion maps in Figure 2. The glia fibre orientation dispersion map is modulated with the volume fraction before it is added to the myelin fibre orientation dispersion values.

Conclusions:

We present a multi-modal comparison of dispersion in the CC estimated from dMRI and measured using microscopy data. A correlation was found in the CC in terms of relative dispersion profiles. A better correlation between dMRI and histology may be ascribed to the fact that water molecules in dMRI experience these structural boundaries observed with high resolution histology, whereas PLI represents more smoothed fibre orientations at slightly lower resolution. Future work will aim to investigate if a simple but robust mapping between these modalities exists.

Imaging Methods:

Diffusion MRI
Polarized light imaging (PLI) [2]

Modeling and Analysis Methods:

Diffusion MRI Modeling and Analysis [1]

Keywords:

Cellular
Glia
Myelin
OPTICAL
White Matter
WHITE MATTER IMAGING - DTI, HARDI, DSI, ETC

[1|2]Indicates the priority used for review

Would you accept an oral presentation if your abstract is selected for an oral session?

Yes

I would be willing to discuss my abstract with members of the press should my abstract be marked newsworthy:

Yes

Please indicate below if your study was a "resting state" or "task-activation" study.

Other

Healthy subjects only or patients (note that patient studies may also involve healthy subjects):

Healthy subjects

Internal Review Board (IRB) or Animal Use and Care Committee (AUCC) Approval. Please indicate approval below. Please note: Failure to have IRB or AUCC approval, if applicable will lead to automatic rejection of abstract.

Not applicable

Please indicate which methods were used in your research:

Optical Imaging
Diffusion MRI
Postmortem anatomy

Which processing packages did you use for your study?

FSL
Other, Please list - Matlab

Provide references in author date format

1. Jbabdi S. & Johanssenberg H. (2010), Tractography, where do we go from here? Brain Connectivity 1:3:169-83
2. Zhang H. et al (2012). NODDI: practical in vivo neurite orientation dispersion and density imaging of the human brain. Neuroimage. 61:4:1000-16
3. Sotiropoulos S.N. et al (2012). Ball and Rackets: Inferring fiber fanning from diffusion-weighted MRI. Neuroimage 60:2:1412-25
4. Budde M.D et al (2013). Quantification of anisotropy and fiber orientation in human brain histological sections. Frontiers in integrative neuroscience. 7:3
5. Mikula S, et al (2012). Staining and embedding the whole brain for electron micrscopy. Nature Methods. 9:12:1198-201.
6. Axer M. et al (2011). High-resolution fiber tract reconstruction in the human brain by mean of three-dimensional polarized light imaging. Frontiers in neuroinformatics. 5:34
7. Marquez J.P. (2006). Fourier analysis and automated measurement of cell and fiber angular orientation distributions. Int. Journal of Solids and Structures. 43:21:6413-23